Proceedings of ALGORITMY 2016
pp. 292–301

NUMERICAL PROPERTIES OF A MODEL PROBLEM FOR EVALUATION OF NATURAL TRACER TRANSPORT IN GROUNDWATER*

MILAN HOKR† AND ALEŠ BALVÍN‡

Abstract. We solve a model problem of natural tracer transport in groundwater between the surface and the tunnel, based on field measured data. The problem with a simplified geometry represents the main features of flow inhomogeneity, namely the presence of fractures and matrix, and an influence of the stagnant zones on the tracer breakthrough. From the fictitious pulse tracer input, we calculate the mean residence time. The problem is solved by the mixed-hybrid finite element method for the flow equation and the discontinuous Galerkin method for the advection-diffusion transport, both implemented in Flow123d open-source software. We check a convergence by the time step refinement and find the limit of the mean residence time with rising time interval. The effect of dispersion parameters can explain some of the differences between results obtained by different numerical software in a separate study [5]. We also show how both the flow and the transport problem have a simple and efficient procedure to solve their inverse problems.

Key words. groundwater, solute transport, advection-diffusion, discontinuous Galerkin, multi-dimensional, fracture, mean residence time, tracer

AMS subject classifications. 65N30, 35R30, 35Q35, 76R99, 86A05

1. Introduction. Many challenges in modelling of groundwater problem are related to inhomogeneity, in particular a combination of high permeable fractures and a less permeable matrix, and to geometry of scale contrasts, e.g. small-scale tunnel/borehole and a large scale transport and hydraulic extent. One of the perspective approaches is a concept of the multidimensional model, coupling subdomains of different dimensions in a single model, requiring non-trivial treatment in mathematical formulation and particular additions in a numerical scheme [3]. Although the theory and numerical solution are on good level of understanding, the concept is not yet routinely used in practical hydrogeological modelling. The Flow123d software [11] developed at the Technical University of Liberec has an ambition to bring the concept into a practice, in particular for the spent nuclear fuel repository safety evaluation, which must be accompanied by verification on both testing and real-world problems.

It is known that for inhomogeneous system (especially with stagnant zones) the tracers breakthrough results to a long tail in the concentration evolution, as the tracer slowly releases from stagnant zones. A related study on a regular schematic model domain is [9]. The characteristic quantity is the tracer residence time. The purpose of this paper is to quantify this effect on a particular case corresponding to real-world conditions and to evaluate how the error of the incomplete mean residence time integral calculation interacts with other numerical effects of temporal discretisation,

*The results were obtained through the financial support of the MŠMT from the project LO1201 in the framework of the targeted support of the "National Programme for Sustainability I". This work has been also supported by TAČR, project code TA04020506 and by SÚRAO, contract code SO2013-077.

†Institute for Nanomaterials, Advanced Technologies, and Innovation, Technical University of Liberec, Czech Republic (milan.hokr@tul.cz).

‡Faculty of Mechatronics, Informatics, and Interdisciplinary Studies, Technical University of Liberec, Czech Republic (ales.balvin@tul.cz).

boundary condition form (related to advection/diffusion ratio), and with solution of an inverse problem, i.e. fitting the rock properties from measured tracers quantities, which is a typical modelling purpose in hydrogeological problems.

The model problem configuration has been suggested in the DECOVALEX-2015 project, aimed on comparison of models and software by various teams. As one of the results, a joint work of the authors of this paper and other teams from Germany and US comparing solution by three different software is currently in progress of submitting [5]. Not all the numerical effects were studied by other teams, which motivated this additional study.

The work also continues previous modelling studies with data from the same site, the water-supply tunnel in granite massif in Bedrichov, Czech Republic. The key steps were the introduction of the multidimensional fracture-matrix concept for the tunnel inflow modelling [6] and the study of the discretisation effects in the scale contrast of the tunnel and the domain [7], all for the water flow equation only.

2. Problem formulation.

2.1. Governing equations. Fluid flow and solute transport in porous media and in fractures are governed by standard equations in literature. For the multidimensional problem, combining the porous medium or the equivalent continuum with the discrete fracture network, we consider the equations separately for each dimensional subdomain Ω_d, $d = 1, 2, 3$, with additional coupling between the dimensions. The problem in a full generality (not used in this study) is described in [2] and in the software documentation [11].

The steady-state flow is governed by the Darcy's law and the mass balance equation

$$\vec{u}_d = -\delta_d K_d \nabla(p_d + z) = -\delta_d K_d \nabla H_d\,, \qquad \mathrm{div}\vec{u}_d = F_d \quad \text{for } d = 1, 2, 3\,, \tag{2.1}$$

where p_d is the pressure head [m], H_d the piezometric head [m] (one of two being the primary unknown), $\vec{u}_d$ is the flux density [$\mathrm{m}^{4-d}\ \mathrm{s}^{-1}$] (secondary unknowns), K_d [$\mathrm{m\ s}^{-1}$] the hydraulic conductivity (scalar in this study, in general tensor), and z the vertical coordinate. The parameters δ_d assure physical compatibility of quantities based on the real geometry: δ_1 is the cross-sectional area of 1D subdomains [m^2], δ_2 is the thickness of 2D subdomains [m], and $\delta_3 = 1$. The source term F_d [$\mathrm{m}^{3-d}\ \mathrm{s}^{-1}$] is composed of the physical sources in the respective subdomain and of a communication with higher-dimension subdomains (for $d = 1, 2$). For detailed expressions we refer to [2, 11], due to technical complexity.

The solute transport is governed by the advection-diffusion equation

$$\frac{\partial(\delta_d n_d c_d)}{\partial t} + \mathrm{div}(\vec{u}_d c_d) - \mathrm{div}(n_d \delta_d D \nabla c_d) = F_d \quad \text{for } d = 1, 2, 3\,, \tag{2.2}$$

where $c_d(\vec{x}, t)$ [$\mathrm{kg\ m}^{-3}$] are the unknown concentrations, n_d are the porosities (dimensionless), D is the hydrodynamic dispersion tensor, and F_d is the source term comprising the physical sources and the subdomains communication. The hydrodynamic dispersion is a total diffusive term composed of the molecular diffusion and the pore-scale mixing, defined by components (we omit d index of the dimension for simplicity):

$$D_{ij} = \delta_{ij} D_m \tau + \|\vec{v}\| \left(\delta_{ij} \alpha_T + (\alpha_L - \alpha_T) \frac{v_i v_j}{\|\vec{v}\|^2} \right)\,, \tag{2.3}$$

where δ_{ij} is the Kronecker delta, D_m the molecular diffusion coefficient, τ the tortuosity, α_L and α_T the longitudinal and transversal dispersivity, and $\vec{v}$ is the average pore velocity [m s^{-1}], which characterize the macroscopic transport. It is related to the flux unknown of the flow problem through the porosity (a transport problem parameter) by

$$\vec{v}_d = \frac{\vec{u}_d}{\delta_d n_d} \,. \tag{2.4}$$

2.2. Problem configuration. The particular study is on a natural tracer transport between surface and a tunnel, to evaluate data sampled in the precipitation and in the tunnel inflow. The problem is defined as an analogue of a real configuration and quantitative conditions, with the only exception in the geometry, when we consider a regular block shape instead of the terrain topography and a general fracture orientation with respect to the tunnel. In Fig.2.1 we show how the solved problem fits to the topography-controlled flow pattern. The second part illustrates the configuration, boundary conditions, and a notation (shallow zone, fracture, matrix).

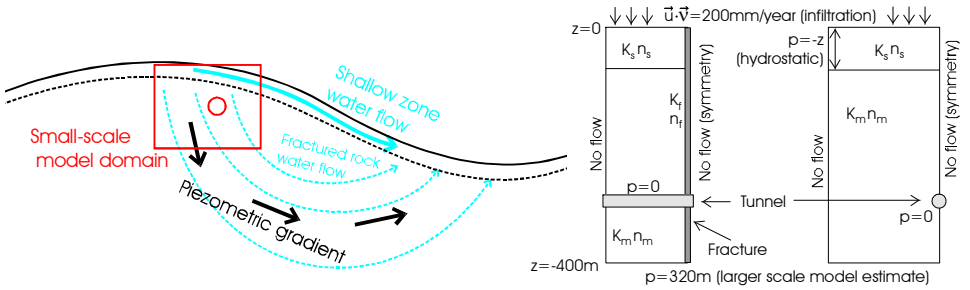

FIG. 2.1. *Problem concept, configuration, and flow boundary conditions (lateral views on the block model domain in two perpendicular directions), the parameter subscripts correspond to the* **s***hallow zone, the* **f***racture, and the* **m***atrix.*

The model of a block shape of 300 m × 100 m × 400 m is composed of three components: the shallow zone where most of the precipitation water is conducted horizontally and drained from the domain (in reality it would be into a stream flow), the vertical fracture capturing the gravitational water flow deeper into the massif (for technical reasons, extended up to the surface along the shallow zone block), and the rock matrix block with very small water flow but a significant storage effect (in reality of this scale, it is an equivalent continuum of several smaller fractures and compact blocks). The represented geometry is one symmetric quarter of the reality.

The steady-state flow is controlled by the set of boundary conditions (Fig.2.1): the Neumann condition of a prescribed infiltration rate (a part of the precipitation), the Dirichlet condition on the outer side of the shallow zone, on the tunnel wall (zero pressure generating the drainage), and on the bottom side of the model generating a piezometric gradient resulting from the larger-scale topography profile. All the conditions are valid for both the surface of the 3D domains and for adjacent line boundaries of the 2D fracture domain, including the transport b.c. below.

The tracer in the model is a fictitious pulse, defined by the concentration $c_{in}(t) = 100$ for $t \in [0, \tilde{t}]$ and $c_{in}(t) = 0$ for $t > \tilde{t}$, where $\tilde{t}$ typically equals to the numerical time step. The only inflow boundary is the upper. There are two options of the tracer injection representation, either as the Dirichlet b.c., $c = c_{in}$ (allowing both advective

TABLE 2.1

Problem parameters for the three model variants corresponding to particular tunnel sampling points. The upper part are measurements fitted in the inverse solution, the lower part are selected variants (former inverse solution, partly fitting the measurement) used as a reference in comparisons.

	Model 2	Model 3	Model 4
tunnel depth [m]	-39.00	-140.00	-91.00
tunnel inflow rate (matrix per 1m) [mL/s]	0.05	5.00E-04	0.05
tunnel inflow rate (2D fracture) [mL/s]	10.00	0.02	14.00
measured mean residence time [month]	42.00	120.00	300.00
K_s (shallow) [m/s]	1.00E-06	1.00E-06	1.00E-06
K_f (fracture) [m/s]	1.03E-07	1.33E-10	2.44E-08
K_m (matrix) [m/s]	4.96E-10	3.27E-12	4.29E-10
n_s (shallow)	0.02	0.02	0.02
n_f (fract)	0.044	4.00E-05	0.073
n_m (matrix)	0.023	4.00E-05	0.073

and diffusive fluxes), or indirectly as the prescribed advective flux, $(\vec{u}c - n\delta D\nabla c)\cdot\vec{\nu} = (\vec{u}\cdot\vec{\nu})c_{in}$. The both approaches tend to be equivalent for an advection-dominated case. The outflow boundary is with the zero Neumann, i.e. the prescribed pure advection (no interaction back into the model domain).

We represent three quantitatively different cases of water inflow – distinguished by depth, flow rate, residence time, and type of the water permeable structure – so the case M2 (i.e. Model 2) is a shallow tunnel section with stronger inflow from a single fracture, M3 is a deep tunnel section with smaller inflow from a single fracture, and M4 is a deep tunnel section with larger inflow from a wider fault structure. The numbering refers to the wider study [5] where also M1 is present representing qualitatively different case of the shallow zone.

The parameters of M2–M4 are listed in Tab.2.1. The remaining parameters are uniform for all the models and all the subdomains: the molecular diffusion coefficient $D_m = 10^{-9}$ m^{2}s^{-1}, the tortuosity $\tau = 0.6$, the longitudinal and transversal dispersivities $\alpha_L = 5$ m and $\alpha_T = 1$ m, leading to dominant dispersion compared to the molecular diffusion in most of the problem domain. Although all the quantities have their physical units, we omit them in most cases below to save space. We always refer to units used in the previous subsection and in the cited table, except the time, which is expressed in months, appropriate with its magnitude.

3. Solution methods.

3.1. Flow and transport numerical schemes. We mainly refer to other literature describing the particular form of the numerical methods. In both cases of the flow and the transport, they are based on generally known principles, adopted to particular configuration of the multidimensional set of subdomains. The flow problem is solved by the mixed-hybrid finite element method, with the lowest-order Raviart-Thomas base functions, piecewise linear for the velocity/flux and piecewise constant for the pressure [1, 3]. The discrete quantities are the pressures in the element centres, pressures in the side centres (the Lagrange multipliers) and fluxes through the element sides (of appropriate dimensions).

The transport problem is solved by the discontinuous Galerkin method [4], which was recently implemented to the Flow123d code, as a follower of the formerly implemented finite volume method, still available as an alternative for problems with pure advection. We use first-order base functions for the concentration and the non-

symmetric variant. The time discretisation is by the implicit Euler method. The details are given in the Flow123d documentation [11].

In both cases, the methods well fit the needs of the problem solution. The mixed-hybrid method provides a conservative velocity field for the subsequent transport calculation and its discrete unknown positions are convenient for the coupling between the different dimensions. The discontinuous Galerkin is one of the options to provide a solution of the advection-dominated problems free of oscillations and with an acceptable numerical diffusion.

3.2. Evaluation of the mean residence time. To get a simple quantity characterising movement of a fluid in a system, a time spent by a tracer particle between the input and the output is often considered. In groundwater, this is typically the time between infiltration (the last contact with the atmosphere) and sampling (here the tunnel).

The set of flow pathways in the system is characterised by the residence time distribution $g(t)$ expressing relative number of pathways with the time of travel equal to t, in the continuous sense [10]. Then the concentration evolution in the output $c(t)$ can be expressed from the input concentration evolution $c_{in}(t)$ by the convolution integral

$$c(t) = \int_0^\infty c_{in}(t-\tau)g(\tau)d\tau\,. \tag{3.1}$$

For a theoretical unit pulse input ($c_{in}(t) = \delta(t)$, the Dirac function), the output evolution is $c(t) = g(t)$. Then the mean residence time (MRT), i.e. the first moment of its density function $g(t)$, can be equivalently evaluated from the transport calculation output as

$$T_{mr} = \frac{\int_0^\infty tc(t)dt}{\int_0^\infty c(t)dt}\,, \tag{3.2}$$

where t is time and $c(t)$ is the concentration in the sampling point, taking into account the input of the total mass other than one or any kind of approximation.

We calculate the MRT by a separate postprocessing of the Flow123d outputs in the spreadsheet, the integrals are evaluated by the rectangle method which is compatible with the integral mass and fluid balance meaning of the solution outputs. There are two main source of the MRT calculation error: the temporal discretisation and the incomplete integral evaluation (approximation by a finite interval of the model simulation time), which are both discussed in the section below. The integral (3.2) is controlled by the residence time distribution $g(t)$ which can be arbitrary function fulfilling $\int_0^\infty g(t)dt = 1$, determined by the system configuration. There are many results in literature describing $g(t)$ and MRT for particular configurations (e.g. [8]), but the approximation behaviour cannot be theoretically predicted for a general case.

4. Model results – parameter sensitivity. The solution evaluated as an evolution of the average concentration in the tunnel–fracture intersection boundary (the breakthrough curve) is basically a non-symmetric peak with a long "tail" of gradual concentration decrease. The curve becomes more symmetric on a logarithmic time axis (Fig.4.1), the three models M2–M4 differ mainly by the position (related to the

TABLE 4.1
Results of the mean residence time for variants of temporal discretisation and the model time interval (all values in time units of months).

		dt=0.4	dt=1	dt=2	dt=10	dt=20
M2	T=600	53.37	53.18	54.13	61.31	
	T=1300	61.63	61.42	62.41	69.61	
	T=10000 (converg.)		74.01		82.5	
M3	T=600	258.87	270.97	258.59	267.38	
	T=6500	643.74	644.02	644.52	654.25	
	T=25000 (converg.)				675.94	
M4	T=600	247.24	248.73	247.75	256.57	263.03
	T=6500	673.17	672.93	673.89	686.31	695.73
	T=20000				963.29	973.09
	T=100000 (converg.)					1139

residence time) and partly qualitatively in the shape. The mean residence time for various cases is listed in Tab.4.1. We study effects of several parameters which are quite free for selection by a user in the application.

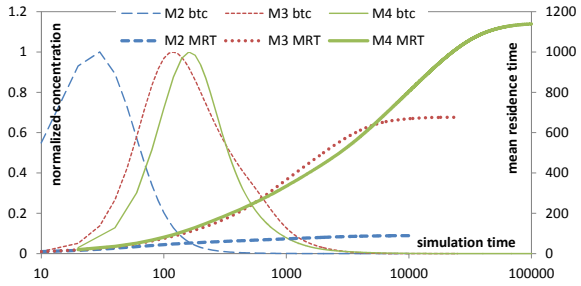

FIG. 4.1. *Breakthrough curves (the tunnel concentration evolution) and the mean residence time depending on the model interval, for the three model variants – the longest calculated intervals with the highest time steps of 10 or 20.*

4.1. Model interval sensitivity. Important and the most insidious is the effect of the model interval as it has no counterpart parameter in the nature. Normally, a criterion for the time interval could be based on a ratio of the inflow and the outflow mass, but it is difficult to define a certain value for this problem because of a dominant part of mass (orders of magnitude ratio) leaving through a different output boundary than the evaluated tunnel sampling point. A more precise evaluation can be done studying a dependence of the evaluated residence time on the model time interval (technically, selecting data from a single long simulation run), as shown in Fig.4.1. The convergence is significantly longer than the value of the mean, confirming the effect of the rock matrix as an almost stagnant zone. Typically, the interval is two orders of magnitude over the MRT and three orders of magnitude over the peak position. The values are also present in a numeric form in Tab.4.1.

4.2. Temporal discretisation. Two effects related to the time step were studied: a check of the convergence with dt decreasing and an effect of coarser dt on the MRT evaluation through an approximation of the Dirac pulse. Visually, the convergence of the breakthrough curve is observed for $dt \leq 0.4$. For all the smaller time steps, the pulse width is the same $\tilde{t} = 2$ for precise comparison. For long interval calculations, larger time steps are necessary, where $\tilde{t} = dt$. The differences in MRT

(Tab. 4.1) due to the time step can be mostly explained by the corresponding shift of the middle of the peak ($\tilde{t}/2$).

4.3. Hydrodynamic dispersion and input boundary effects. The hydrodynamic dispersion parameters are very difficult to determine in practice and usually they are chosen in relation to the model scale. We study their effect on the model evaluation for this reason, to see the related uncertainty. There are four values of dispersivities around the reference one, covering a range of three orders of magnitude, from $\alpha_L = 0.05$ and $\alpha_T = 0.01$ to $\alpha_L = 50$ and $\alpha_T = 10$. The results for M2 and M3 are presented in Fig.4.2. The two lowest dispersion cases are relatively close to each other, meaning a small contribution of the equation term to the overall diffusion/dispersion process. As the decrease of the molecular diffusion coefficient did not have significant effect, we assign the pulse smearing to the "macro-dispersion", the mixing between permeable and stangant zones.

While the dispersion has a strong effect on the mean residence time (known also for 1D advection-diffusion), the choice of the injection boudnary condition has a smaller effect on MRT within the range of uncertainty of time discretisation, compared to relatively more visible peak shape differences (4.2).

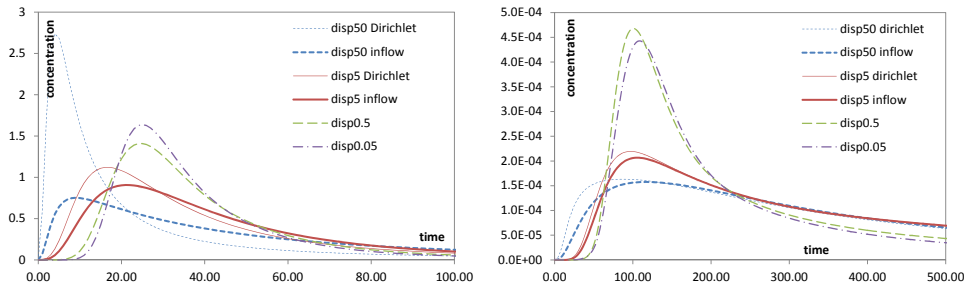

FIG. 4.2. *Sensitivity of the problems on the dispersivity parameters α_L and α_T (the former put into the legend, while the latter scaled in the same ratio), M2 in the left and M3 in the right. The solid(=red) line is the reference case. The effect of the injection boundary condition is not visible for the two cases with the dominant advection.*

5. Inverse problem solution. The problem has been solved as an inverse problem, both for the flow and for the transport part. For the former, it means finding the hydraulic conductivities K_f and K_m fitting the measured inflow into the tunnel from the fracture and from the matrix respectively. For the transport, it means finding the porosities of the subdomains (shallow, fracture, and matrix), fitting the given residence time.

5.1. Measured data. The tunnel inflow is measured in several sampling points and in a canal collecting all the water along the tunnel. The sampling points, typically in larger fractures and faults, correspond to the fracture inflow in the model. The matrix inflow is so small that it cannot be measured directly and the rate is derived indirectly from the canal flow rate change along the position, with less accuracy. The inflow from the shallow zone is also derived from the canal flow rate and it was used to estimate the shallow zone hydraulic conductivity K_s (considered as a given parameter in this study).

The mean residence time is not measured directly but it is derived from natural tracers concentrations. The data in the background of this study are from stable

isotopes ^{2}H and ^{18}O in the water molecule and from tritium ^{3}H and its decay product ^{3}He in a form of dissolved gas. In the latter case, the time between infiltration input and the tunnel output can be calculated from the decay rate. For the stable isotopes, the mean residence time is obtained as a parameter in a lumped parameter model, as an inverse problem solution, fitting the temporal concentration evolution in the tunnel related to the given input evolution in the atmosphere.

The particular data to be fitted are in the upper part of Tab. 2.1. The transport problem inversion below needs additional conditions obtained from physical arguments: The shallow zone tracer breakthrough should be similar for all model cases and the mean residence time derived at another tunnel sampling point in the shallow zone can be seen as partial residence time T_s in the shallow subdomain (explained below). Similar, we can apply a-priori estimates on the rock matrix porosity (a parameter) – equality between the models and a range of literature values based on laboratory sample measurements. For demonstration purposes with one model only, the conditions are introduced in the form of two synthetic residence time values T_f and T_m (the rightmost column of Tab. 5.1).

5.2. Flow problem. The inverse hydraulic problem has convenient properties that the fracture inflow is dominantly controlled by the fracture conductivity and the matrix inflow by the matrix conductivity, but not exclusively. The dependence is approximately linear, resulting from the equation linearity (valid fully for a homogeneous problem only). The iterations to the inverse solution can therefore be based on this property – the new estimate of $K_i^{(k+1)}$ is derived from the current $K_i^{(k)}$ and the ratio between the current flux solution $Q_i^{(k)}$ and the measurement $Q_i^{(meas)}$, for $i \in \{f, m\}$ (the fracture and the matrix):

$$K_i^{(k+1)} = K_i^{(k)} \frac{Q_i^{(meas)}}{Q_i^{(k)}} \,. \tag{5.1}$$

The ratio between a sensitivity of the flux on the corresponding subdomain conductivity and on the second subdomain conductivity is about two orders of magnitude. The convergence is therefore very quick, decreasing the error by such ratio each step. Usually two iterations are enough for practical model calibration precision. Also, the same number of parameters and constraints (together with the quasi-linearity) means that the problem has a unique solution. Examples for the particular models are given in Fig.5.1.

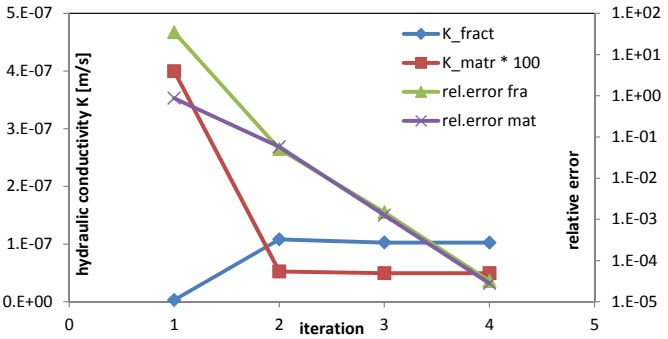

FIG. 5.1. *Iterations of the flow inverse problem solution – K parameter values and the error.*

TABLE 5.1
Iterations of the transport model inverse algorithm and the fitted residence time values.

	init	iter1	iter2	iter3	fitted time
n_s	0.1	0.027	0.0263	0.0264	T_s= 30.59
n_f	0.05	0.0225	0.0219	0.0221	T_f= 4
n_m	0.01	0.005	0.0041	0.004092	T_m= 8
MRT	138.33	44.96	42.43	42.58	T_{mr}= 42.59
relative error	2.25	5.55E-02	-3.80E-03	-1.40E-04	

5.3. Transport problem. The inverse transport problem has similar property of the linearity but not the equal number of parameters and constraints. Typically, the inverse problems are solved as overdetermined, solving an optimization problem minimizing the error (residual). Here we have an underdetermined problem, with three parameters (porosities) and one constraint condition of the mean residence time, so the problem was completed with physical assumptions in the section 5.1.

To apply the information on the shallow zone residence time, we need additional understanding of the problem properties. The total residence time T_{mr} can be split into partial residence times in subdomains, by analogue to "serially" connected segments

$$T_{mr}(n_i) = \sum_i T_i = \sum_i \frac{L_i}{v_i} = \sum_i n_i \frac{L_i}{u_i}\,, \tag{5.2}$$

where L_i are the segment lengths, v_i are the transport velocities, and u_i are the flux densities (given from the hydraulic model).

In our 3D case, we use the above equation as an approximation, for the three subdomains $i \in \{s, f, m\}$. The unknown factors L_i/u_i at the porosities are evaluated as derivatives $T_i^{(app)} = \frac{\partial T_{mr}}{\partial n_i} n_i$ and approximated by perturbation sensitivities (i.e. forward difference formulas) with 1% change of n_i. Then the k-th iteration is defined

$$n_i^{(k+1)} = n_i^{(k)} \frac{T_i^{(meas)}}{T_i^{(app,k)}} = T_i^{(meas)} \left[\frac{\partial T_{mr}}{\partial n_i} \alpha^{(k)} \right]^{-1}\,, \tag{5.3}$$

where an additional correction factor is used, defined by $\alpha^{(k)} \sum_{i\in\{s,f,m\}} \frac{\partial T_{mr}}{\partial n_i} n_i = T_{mr}$, corresponding to the property that T_{mr} is proportional to a uniform change of porosity in the whole domain. This is especially important for the MRT approximation by an incomplete integral to get more realistic values.

The solution for given subdomain residence times is an analogue of the hydraulic inverse problem, but with less separated parameter sensitivity. An example for M2 is given in Tab.5.1, with the convergence rate of one order of magnitude every time step.

6. Conclusion. We studied several properties of a flow and transport model problem used for evaluation of the natural tracer data sampled in a tunnel, to determine the water mean residence time and estimating porosities as some of the rock parameters. We found that the simulation length is much more important than temporal discretisation to get reasonable results of MRT. Especially for repeated calculations during an inverse solution, it is convenient to use relatively long time steps to save computing time and then to switch to a smaller time step in the last iteration.

Also, the form of the injection boundary condition, which is usually not subject of attention, can significantly influence the shape of the breakthrough curve and partly

the mean residence time, for problems not strictly advection-dominated. Moreover, we could see that diffusion/dispersion parameters control not only the breakthrough curve width (tracer spreading) but also the peak position and MRT, masking the expected effect of advective velocity.

The inverse problem solution based on the specific problem properties and on the physical understanding was found efficient and the practical experience confirms it as an alternative to general-purpose methods.

A following work of fitting a general tracer concentration evolution sampled both in the precipitation and in the tunnel is in progress, as a direct approach avoiding the intermediate use of the lumped parameter models and the pulse tracer evaluation [10]. This leads to an inverse problem more complicated to solve, but with a stronger determination by the data, allowing to estimate also the dispersion parameters, additional to the porosities related to the advection.

Acknowledgments. The work described in this paper was conducted within the context of the international DECOVALEX Project (DEmonstration of COupled models and their VALidation against EXperiments). The authors are grateful to the Funding Organisation who supported the work. The views expressed in the paper are, however, those of the authors and are not necessarily those of the Funding Organisations. The authors thank to H. Shao from the Federal Institute for Geosciences and Natural Resources (Germany) and W.P. Gardner from the Sandia National Laboratories (USA) for their participation on the model problem formulation.

REFERENCES

[1] F. Brezzi and M. Fortin, *Mixed and hybrid finite element methods*. Springer, New York, 1991

[2] J. Březina, M. Hokr, *Mixed-Hybrid Formulation of Multidimensional Fracture Flow* In: Numerical Methods and Applications, Lecture Notes in Computer Science Volume 6046, 2011, pp 125-132.

[3] J. Březina, *Mortar-Like Mixed-Hybrid Methods for Elliptic Problems on Complex Geometries*, In: D. Ševčovič, A. Handlovičová, Z. Minarechová, editor, ALGORITMY 2012 - 19th Conference on Scientific Computing, Slovak University of Technology in Bratislava, Publishing House of STU, 2012.

[4] A. Ern, A. F. Stephansen, and P. Zunino, *A discontinuous Galerkin method with weighted averages for advectiondiffusion equations with locally small and anisotropic diffusivity*, IMA Journal of Numerical Analysis, 29(2) (2009), 235-256.

[5] M. Hokr, H. Shao, W.P. Gardner, A. Balvín, H. Kunz, Y. Wang, M. Vencl, *Real-case benchmark for flow and tracer transport in the fractured rock*, In preparation, to be submitted to Envir. Earth Sci., 2015

[6] M. Hokr, I. Škarydová, and D. Frydrych, *Modelling of tunnel inflow with combination of discrete fractures and continuum. Computing and Visualization in Science*, 15(1) (2013), pp.21-28.

[7] M. Hokr, A. Balvín, D. Frydrych, I. Škarydová, *Meshing issues in the numerical solution of the tunnel inflow problem*, In: Mathematical Models in Engineering and Computer Science (Marascu-Klein, ed.), NAUN, 2013, pp. 162-168

[8] H.A. Loáiciga, *Residence time, groundwater age, and solute output in steady-state groundwater systems*, Adv. Water Res. 27 (2004), 681–688.

[9] P. Maloszewski and A. Zuber, *On the Theory of Tracer Experiments in Fissured Rocks with a Porous Matrix*, Journal of Hydrology, 79 (1985), 333–358.

[10] A. Suckow, *The age of groundwater – Definitions, models and why we do not need this term*, Applied Geochemistry, 50 (2014), 222–230.

[11] TUL, *Flow123d version 1.8.2, Documentation of file formats and brief user manual*, Technical University of Liberec, 2015, Online: http://flow123d.github.io/.